

Climate sensitive single tree growth modeling using a hierarchical Bayes approach and integrated nested Laplace approximations (INLA) for a distributed lag model

Arne Nothdurft

University of Natural Resources and Life Sciences, Vienna (BOKU), Austria, Department of Forest- and Soil Sciences, Institute of Forest Growth



ARTICLE INFO

Keywords:

Forest growth model
Tree-ring width analysis
Distributed lag model
Hierarchical Bayes model
INLA
Climate sensitivity
Species mixing

ABSTRACT

A novel methodological framework is presented for climate-sensitive modeling of annual radial stem increments using tree-ring width time series. The approach is based on a hierarchical Bayes model together with a distributed time lag model that take into account the effects of a series of monthly temperature and precipitation values, as well as their interactions. By using a set of random walk priors, the hierarchical Bayes model allows both the detrending of the individual time series and the regression modeling to be performed simultaneously in a single model step. The approach was applied to comprehensive tree-ring width data from Austria collected on sample plots arranged in triplets representing different mixture types. Bayesian predictions revealed that European larch (*Larix decidua* Mill.), Norway spruce (*Picea abies* (L.) H. Karst.), and Scots pine (*Pinus sylvestris* L.) show positive climate-related growth trends throughout higher elevation sites in Tyrol, and these trends remain unchanged under a mixed-stand scenario. At the lower Austrian sites, Norway spruce was found to show a severely negative growth trend under both the pure- and mixed-stand scenario. The increment rates of European beech (*Fagus sylvatica* L.) were found to have a negative climate-related trend in pure stands, and the trend diminished through an admixture of spruce or larch. The trends of European larch and sessile oak (*Quercus petraea* (Matt.) Liebl.) showed stationary behavior, irrespective of the mixture scenario. Scots pine data showed a positive trend at the lower elevation sites under both the pure- and mixed-stand scenario. These findings indicate that species mixing does not lower the climate-related increment fluctuations of beech, oak, pine, and spruce at lower elevation sites.

1. Introduction

Single tree productivity rates are influenced by a complex array of intrinsic and extrinsic factors (Fritts, 1976). Presently, climate has come into special focus in tree productivity research, especially in the context of recent discussions on the outcomes of global warming. Although evidence has been found that productivity rates in Central European forest ecosystems have generally increased during the last century (Pretzsch et al., 2014), it is very likely that these trends will not continue in the future. This is mainly because climate projections suggest there will be higher frequencies and intensities of heat waves (Beniston et al., 2007) together with rainfall shifts from summer to winter months (Rajczak et al., 2013; Gobiet et al., 2014). Given these climate projections, higher frequencies and longer durations of drought periods become very likely (Jacob et al., 2014). Because transpiration and net photosynthesis exhibit severe declines as a consequence of drought (Leuzinger et al., 2005; Bréda et al., 2006; Timofeeva et al., 2017), productivity losses are rather expected for future periods (Vitali et al.,

2018a; Vitasse et al., 2019). Hence, an in-depth understanding of the climate-growth relationships nowadays is crucial to providing credible long-term prognoses of potential forest growth.

Forest growth models have been traditionally built by using data from repeated measures inventories with long intervals of several years between two consecutive surveys; an example of such a successful implementation can be seen in the work of Monserud and Sterba (1996) in Austria. In fact, seasonal xylem formation and annual productivity rates are determined by short-term climate fluctuations (e.g., Oberhuber and Gruber (2010), and references therein). Hence, it is hardly possible to reveal the climate-growth relationships by using repeated measures survey data, and tree-ring analysis is nowadays preferred instead (van der Maaten-Theunissen et al., 2016).

The xylem formation is not only influenced by the current year's climate conditions, but also by time-lagged effects of longer climate sequences in the past (Castagneri et al., 2018). Consequently, "drought legacy effects" of the precedent year lower the tree-ring width increments by 10%, according to the findings in Kannenberg et al. (2019).

E-mail address: arne.nothdurft@boku.ac.at.

<https://doi.org/10.1016/j.foreco.2020.118497>

Received 12 May 2020; Received in revised form 30 June 2020; Accepted 8 August 2020

Available online 07 September 2020

0378-1127/© 2020 The Author. Published by Elsevier B.V. This is an open access article under the CC BY-NC-ND license (<http://creativecommons.org/licenses/by-nc-nd/4.0/>).

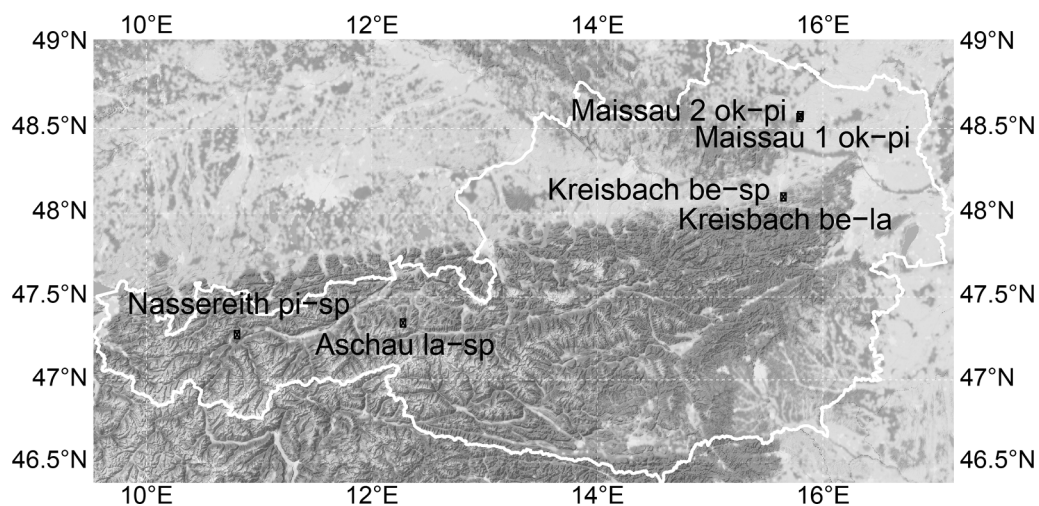


Fig. 1. Locations of the triplet plots in Austria.

Prior to death, trees show more drastic growth decreases after drought and frost (Vanoni et al., 2016). However, the possible symptoms of growth decline can even lag several years behind the extreme climate event (Bréda and Badeau, 2008).

The growth reactions of trees to such climate extremes generally differ among tree species; for example, the growth of larch and spruce is more influenced by spring droughts than that of oak and silver fir (Vitasse et al., 2019). In addition, a mixing situation in the neighborhood can likewise modify productivity rates in drought years. This was demonstrated in Vitali et al. (2018b), in which a mixed-species constellation in the neighborhood was found to be favorable for silver fir but not for Douglas fir, and it had either a positive or negative effect for Norway spruce, which was dependent on the stem density and the other species in the neighborhood.

Furthermore, drought reactions and possible legacy effects are preconditioned by other forest site characteristics. It was found in Trouvé et al. (2017) that trees at dry sites showed faster recovery rates than those at moister sites. For ponderosa pine and trembling aspen in the southwestern USA, a higher level of water stress and stronger growth decline was observed at lower elevation sites (Anderegg and HilleRisLambers, 2016).

In this study, novel methodology is presented for the quantification of climate influences on the radial stem increments of single trees. Based upon the fundamentals presented in Nothdurft and Vospernik (2018) and Nothdurft and Engel (2020), a distributed lag model was used to consider time-lagged climate effects on annual increment rates. Thus far, I have approached the statistical inference from a frequentist perspective by using a generalized additive model (GAM) setting. In fact, the GAM approach with penalized smoothing splines has proven to be very flexible, as it allows for the consideration of interactions of nonlinear effects. However, this approach presents major drawbacks, e.g., model fitting is computationally costly, model behavior is sensitive to the degree of smoothing, and uncertainty quantification is not straightforward. Hence, a novel statistical framework was constructed here in the form of a hierarchical Bayes model. In this respect, my work was inspired by Foster et al. (2016) and Iter et al. (2017, 2019), who have presented Bayesian inferential techniques for the analysis of dendrochronological data.

Fully Bayesian inference from the posterior is traditionally derived via Markov chain Monte Carlo (MCMC) simulation techniques (Metropolis et al., 1953; Hastings, 1970; Gelfand and Smith, 1990). However, this is computationally expensive and hinders an iterative model building process, which necessarily implies the re-running, checking, and exploration of alternative model candidates. To circumvent these problems, I used the Integrated Nested Laplace Approximations (INLA) (Rue et al., 2009; Martins et al., 2013) method as an

alternative to MCMC, which allowed for both fast and accurate computations. For the computations, I used routines that were implemented in the R-INLA package (Lindgren and Rue, 2015).

Tree-ring width data for different tree species were derived from sample plots in Austria to examine whether climate-related growth trends differ between pure and mixed stand situations as well as between low and high elevation sites. It was hypothesized that growth trends at lower and higher elevation sites will show opposite signs, with clear positive trends at the high elevation sites. More specifically, I assumed that spruce would show negative trends at low elevation sites, whereas other more drought tolerant species would at least display stationary trends. It was expected that a mixed species neighborhood would weaken the growth trends and also reduce the climate-related fluctuations of the annual stem diameter increments.

2. Materials and methods

2.1. Survey plots

Sample plots were established in a triplet design to study the effects of species mixing on the increment rates and tree resistance to climate extremes. That is, a particular triplet was comprised of a single sample plot in a mixed stand with two species and two further plots that were placed in pure stand situations for both species. Data were analyzed from in total six triplets in Austria. Hereof, four triplets were located at lower elevation sites in the federal state of Lower Austria nearby Kreisbach (487 m above sea level, a.s.l.) and Maissau (436 and 388 m a.s.l.), and two triplets were located at higher elevations in the state of Tyrol nearby Aschau (1570 m a.s.l.) and Nassereith (973–1055 m a.s.l.); see Fig. 1 and Table 1.

Two triplets were installed at the Maissau site, both with the same tree species combination of sessile oak (*Quercus petraea* (Mattuschka) Liebl.) and Scots pine (*Pinus sylvestris* L.). Given that usual forest management activities will be conducted at Maissau 1, the Maissau 2 triplet was treated as an unmanaged control variant in the future. At the Kreisbach site, one triplet was for the combination of European beech (*Fagus sylvatica* L.) and European larch (*Larix decidua* Mill.) and the other triplet was for European beech and Norway spruce (*Picea abies* (L.) H.Karst.). European larch and Norway spruce also grew at the Aschau triplet, and Scots pine and Norway spruce grew at the Nassereith triplet. Measurement campaigns on the Maissau and Nassereith triplet plots were initiated within the European-wide project “REFORM” (<http://www.reform-mixing.eu/>). REFORM’s major goal is to formulate mixed-species forest management options that increase the resilience of forest ecosystems and lower the risk of possible climate change impacts.

Table 1

Summary characteristics of the sample plot data. Elevation above sea level in meter units (elev.), sample plot area in hectares (area, ha), stem density as the number of trees per hectare (N), basal area in m²/ha (BA), DBH is the diameter at breast height in centimeter units, and height is the tree height in meter units.

site	plot	elev.	area	N	BA	DBH (cm)				height (m)				species 1			species 2		
						mean	sd	min	max	mean	sd	min	max	Sp 1	N	BA	Sp 2	N	BA
Aschau la-sp	mixed	1570	0.62	691	74.7	34.4	13.9	3.4	77.5	27.1	8.3	2.6	36.6	larch	176	24.1	spruce	509	50.1
	larch	1570	0.82	465	39.4	29.9	13.6	5.6	72.5	25.8	8.6	1.2	34.4						
	spruce	1570	0.50	773	78.7	33.5	13.3	5.6	85.3	26.4	7.8	3.1	42.9						
Kreisbach be-la	mixed	487	0.54	514	51.1	33.9	10.9	6.5	63.3	35.4	5.9	3.4	43.5	beech	431	39.7	larch	64	9.5
	beech	487	0.19	695	51.1	29.3	9.0	14.1	65.9	33.3	4.5	19.5	37.3						
	larch	487	0.36	959	52.6	24.3	10.3	5.8	55.9	27.8	6.6	7.0	34.4						
Kreisbach be-sp	mixed	487	0.67	512	42.3	32.0	10.7	9.1	68.0	24.4	5.4	4.4	38.5	beech	307	20.9	spruce	150	15.9
	beech	487	0.19	734	40.0	27.3	8.1	8.0	50.3	25.7	5.2	10.7	35.5						
	spruce	487	0.22	478	54.7	38.4	8.6	13.4	62.3	25.8	3.0	15.7	34.3						
Maissau 1 ok-pi	mixed	436	0.21	623	31.8	24.1	8.5	6.2	57.4	21.3	4.2	5.1	25.1	oak	258	16.0	pine	311	14.3
	oak	436	0.22	441	25.6	23.0	14.5	5.1	48.9	21.4	7.5	4.2	28.2						
	pine	436	0.14	1178	40.6	20.2	5.4	5.1	34.5	20.1	3.4	4.2	24.9						
Maissau 2 ok-pi	mixed	388	0.55	428	30.3	28.3	9.9	5.5	61.4	20.3	4.5	2.0	26.7	oak	183	16.1	pine	210	13.3
	oak	388	0.29	285	26.5	33.5	8.2	11.3	51.6	19.4	2.9	8.3	25.4						
	pine	388	0.22	728	39.6	25.8	5.3	7.0	42.3	20.7	3.3	2.0	25.9						
Nassereith pi-sp	mixed	973	0.51	410	47.0	34.5	16.4	5.4	73.0	30.7	10.4	3.4	40.3	pine	96	16.9	spruce	271	19.1
	pine	889	0.34	1088	42.4	21.6	5.5	5.9	37.5	18.9	3.2	4.0	24.9						
	spruce	1055	0.15	565	44.7	30.3	9.6	5.9	54.3	26.3	6.8	4.1	34.8						

2.2. Climate data

The climate data were derived from the HISTALP dataset (Böhm et al., 2009). For each triplet location, monthly averages of atmospheric temperature and monthly totals of precipitation were obtained via spatiotemporal interpolations with generalized additive models; see Nothdurft and Vospernik (2018) and Nothdurft and Engel (2020) for further details. The long-term average annual temperature during 1950–2017 was lower at the Tyrolean sites Aschau (2.0 °C) and Nassereith (5.5 °C) than that at the Lower Austrian sites Kreisbach and Maissau, where a value of 7.4 °C was observed at both sites (see Table 2). The interquartile range (IQR), i.e., the difference between the 3rd and 1st quartile, of the average annual temperature was wider in Tyrol (2.1 kelvin (K) in Aschau, 1.9 K in Nassereith) than that in Lower Austria (1 K). At all four sites, the average monthly temperatures were hottest in July with values of 11.6 °C in Aschau, 15.1 °C in Nassereith, and 17.0 °C in Kreisbach and Maissau. January had the coldest average temperature with values of −7.9 °C in Aschau, −4.4 °C in Nassereith, and −2.5 °C in Kreisbach and Maissau.

The average total monthly precipitation was higher at the Tyrolean sites (1072 mm in Aschau and Nassereith 1038 mm) than that at the Lower Austrian sites (see Table 3). The average total annual precipitation was 812 mm in Kreisbach and 551 mm in Maissau. While temperatures were similar at both sites in Lower Austria, the climate in Kreisbach was more humid than that in Maissau. The IQR of the average total annual precipitation was similarly high at the Aschau, Kreisbach, and Nassereith sites (132, 146, and 144 mm), and it was lower at the Maissau site (108 mm). The highest monthly rainfall generally occurred in July, but precipitation at the Maissau site was highest in June. The lowest precipitation occurred in February throughout all of the study sites.

2.3. Tree-ring data

Tree-ring cores were generally collected from 30 trees per species in the sample plots, of which 20 randomly selected trees had a dominant social status and 10 trees had a subdominant status. However, a few sample cores were irreparably damaged; thus, extra trees were sampled

as a reserve. Ultimately, tree-ring measurements from a minimum number of 28 and a maximum number of 32 trees per species in the sample plots were available (see Table 4). In fact, two wood cores were extracted per sample tree at breast height (1.3 m above ground) by using an increment borer. The cores were drilled in the radial direction toward the pith, one from the north direction and the other from south direction. The tree-ring width measurements of both cores were finally averaged per calendar year. On average, between 42 and 122 tree-ring width observations were available per sample tree, species, and plot. The average number of observations on the Aschau, Maissau2, and Nassereith plots was higher than that on the plots in Kreisbach and Maissau1. This was because tree ages on the former plots were older than those on the latter plots.

2.4. Model construction

In accordance with my prior experiences, I assumed that the response variable tree-ring width y was gamma-distributed with density

$$\pi(y) = \frac{b^a}{\Gamma(a)} y^{a-1} \exp(-by), \quad a > 0, \quad b > 0, \quad y > 0$$

having the expectation $\mathbb{E}(y) = \mu = a/b$ and variance $\text{Var}(y) = 1/\tau_1 = a/b^2$. Parameter τ_1 , the inverse variance, is termed the precision, and the R-INLA package used

$$\tau_1 = (s\phi)/\mu^2$$

for its parameterization. With the new precision parameter ϕ and fixed scaling $s = 1$, the reformulated gamma density became

$$\pi(y) = \frac{1}{\Gamma(\phi)} \left(\frac{\phi}{\mu} \right)^\phi y^{\phi-1} \exp\left(-\phi \frac{y}{\mu}\right).$$

The precision parameter ϕ was a hyperparameter, which was represented as $\phi = \exp(\theta_1)$. A diffuse log-gamma prior was defined on θ_1 .

It was further assumed that the linear predictor η_i for the ring-width measurements y_i of tree i was linked to the mean μ via a logarithmic link

$$\log[\mathbb{E}(y_i)] = \log(\mu) = \eta_i.$$

Table 2

Summary statistics of the average annual (year) and the average monthly temperature (Jan–Dec) in °C units at the study sites during 1950–2017 in terms of the minimum (min), 1st quartile (1st quart), mean, 3rd quartile (3rd quart), and maximum (max).

	year	Jan	Feb	Mar	Apr	May	Jun	Jul	Aug	Sep	Oct	Nov	Dec	
Aschau	min	-4.0	-17.9	-17.1	-9.0	-3.2	0.4	4.9	6.5	4.7	2.3	-3.9	-8.4	-15.0
	1st quart	1.1	-9.1	-8.1	-4.8	0.3	4.9	8.6	10.3	9.6	6.3	1.7	-4.2	-8.2
	mean	2.0	-7.9	-6.4	-2.9	1.8	6.3	9.8	11.6	10.8	7.4	2.3	-2.6	-6.7
	3rd quart	3.2	-6.4	-4.3	-0.7	3.3	8.0	11.3	13.1	12.0	9.0	3.5	-0.9	-4.9
	max	5.6	-2.6	-1.5	2.4	6.1	10.1	14.4	16.9	15.5	11.4	7.4	2.7	-1.5
Kreisbach	min	5.9	-7.8	-9.6	-1.8	3.9	7.1	12.0	14.4	13.6	9.9	4.0	-0.3	-5.7
	1st quart	6.8	-3.5	-2.5	1.1	6.2	10.7	14.4	15.9	15.3	12.2	6.9	1.8	-2.5
	mean	7.4	-2.5	-0.9	2.6	7.2	11.7	15.3	17.0	16.2	12.8	7.8	2.8	-1.2
	3rd quart	7.8	-1.2	1.1	4.3	8.2	12.6	15.8	18.0	16.9	13.5	8.7	3.7	0.1
	max	9.5	2.5	3.5	6.2	10.6	14.9	19.3	21.0	19.8	15.0	11.3	6.5	2.6
Maissau	min	5.6	-7.6	-9.7	-1.9	4.2	7.1	12.2	14.0	13.8	9.5	3.6	-0.4	-6.0
	1st quart	6.8	-3.7	-2.6	1.1	6.3	10.7	14.5	16.2	15.3	12.2	6.9	1.7	-2.4
	mean	7.4	-2.5	-1.0	2.5	7.2	11.7	15.2	17.0	16.2	12.8	7.7	2.8	-1.3
	3rd quart	7.8	-1.3	1.2	4.2	8.1	12.6	16.0	17.8	17.0	13.5	8.5	3.7	0.0
	max	9.3	2.4	3.6	6.0	10.5	14.6	18.8	20.9	20.5	14.9	11.2	6.3	2.5
Nassereith	min	-3.5	-17.4	-16.6	-8.5	-2.4	1.4	5.5	7.1	6.8	2.8	-1.4	-5.1	-14.5
	1st quart	4.4	-5.7	-4.6	-1.3	3.9	8.2	12.0	13.8	13.4	9.9	5.1	-0.7	-4.6
	mean	5.5	-4.4	-2.9	0.6	5.3	9.7	13.3	15.1	14.3	10.9	5.8	0.9	-3.2
	3rd quart	6.3	-3.2	-0.9	2.8	6.7	11.4	14.8	16.6	15.3	12.2	6.9	2.6	-1.4
	max	10.0	1.8	2.9	6.8	10.0	13.9	18.8	21.0	19.6	15.3	11.3	7.1	2.6

The linear predictor was constructed as follows

$$\eta_i = f_i(\text{Age}_i) + \sum_{k=1}^l \gamma_k \cdot \text{Temp}_{ik} + \sum_{k=1}^l \delta_k \cdot \text{Prec}_{ik} + \sum_{k=1}^l \kappa_k \cdot \text{Temp}_{ik} \cdot \text{Prec}_{ik} + \mathbf{u}_i + \epsilon_i. \quad (1)$$

Its first component $f_i(\text{Age}_i)$ performed an individual detrending of each tree-ring width series. The following three sum terms represented a distributed lag model and accounted for the effect of climate in terms of monthly average temperatures and monthly total precipitation amounts as well as their interactions. The last term among the relevant components was \mathbf{u}_i , a tree-level random effect.

The individual detrending was achieved with second-order random walks (RW2)

$$\nabla^2 f_i(\text{Age}_{i,j}) = f_i(\text{Age}_{i,j}) - 2f_i(\text{Age}_{i,j-1}) + f_i(\text{Age}_{i,j-2}), \quad j = 3, \dots, n_i$$

Table 3

Summary statistics of the total annual (year) and the total monthly precipitation (Jan–Dec) at the study sites in mm units during 1950–2017 in terms of the minimum (min), 1st quartile (1st quart), mean, 3rd quartile (3rd quart), and maximum (max).

	year	Jan	Feb	Mar	Apr	May	Jun	Jul	Aug	Sep	Oct	Nov	Dec	
Aschau	min	750	3	6	8	6	10	67	49	74	33	1	0	8
	1st quart	1003	33	23	37	50	75	112	124	112	69	38	40	38
	mean	1072	63	50	62	71	101	138	153	142	92	71	65	63
	3rd quart	1135	88	66	82	92	122	161	175	163	112	94	87	79
	max	1464	180	167	176	130	202	259	323	260	181	200	211	193
Kreisbach	min	559	6	4	12	3	23	24	28	36	11	1	0	5
	1st quart	742	28	24	34	36	57	69	72	67	44	30	36	35
	mean	812	44	42	54	58	86	103	108	94	70	52	53	48
	3rd quart	888	58	54	68	75	105	128	134	114	84	73	68	57
	max	1170	118	120	138	159	242	312	254	255	212	154	115	100
Maissau	min	359	2	1	6	1	12	22	16	13	3	1	1	5
	1st quart	495	15	13	19	20	46	50	51	41	28	17	23	18
	mean	551	26	25	34	40	65	78	74	66	46	34	36	29
	3rd quart	603	34	37	46	55	80	96	89	79	56	45	44	39
	max	774	59	72	102	99	142	164	167	221	136	102	90	81
Nassereith	min	760	4	9	10	7	11	60	48	42	28	1	0	5
	1st quart	961	37	27	37	49	71	113	115	107	64	38	43	36
	mean	1038	58	50	59	70	99	130	142	141	92	68	67	61
	3rd quart	1105	79	63	74	94	126	146	159	161	119	95	87	75
	max	1362	168	170	172	137	185	229	242	236	193	161	157	148

across the n_i ring-width measurements of tree i . By doing so, it was assumed that the $n_i - 2$ second-order differences of each tree-ring series were independently and normally distributed

$$\nabla^2 f_i(\text{Age}_{i,j}) \sim N(0, \tau_2^{-1})$$

across the ordered age sequence. The density for the smooth function values $f_i(\text{Age}_i)$ of each tree-ring series followed a multivariate Gaussian distribution

$$\pi(f_i(\text{Age}_i) | \tau_2) \propto \tau_2^{(n_i-2)/2} \exp\left\{-\frac{1}{2} f_i(\text{Age}_i)^T Q_2 f_i(\text{Age}_i)\right\},$$

where $Q_2 = \tau_2 R_2$ and

Table 4

Summary characteristics of the sample trees.

site	mixture	species	trees	No. of obs.			age				DBH (cm)				height (m)				
				mean	sd	min	max	mean	sd	min	max	mean	sd	min	max	mean	sd	min	max
Aschau la-sp	mixed	larch	28	101	14.8	75	130	101	15	75	130	40.0	12.1	8.4	58.7	30.6	5.3	9.3	35.9
	mixed	spruce	31	77	16.4	44	117	77	16	44	117	35.9	10.3	17.3	65.2	22.2	4.5	12.0	31.8
	pure	larch	30	122	18.1	82	160	122	17	96	160	39.6	10.3	13.4	63.4	26.7	4.3	15.3	34.4
	pure	spruce	28	71	7.2	56	92	71	7	56	92	41.9	8.7	28.9	64.2	26.8	3.0	20.2	32.5
Kreisbach be-la	mixed	beech	32	79	4.1	71	89	79	4	71	89	39.6	10.3	16.9	63.3	34.7	3.9	22.4	39.3
	mixed	larch	29	78	3.6	69	86	78	4	68	86	41.7	7.1	29.4	54.0	36.3	3.2	29.8	41.6
	pure	beech	30	71	7.5	41	77	71	7	41	77	35.8	8.2	15.2	46.4	33.3	4.0	19.5	37.3
	pure	larch	30	67	1.9	61	70	67	2	61	70	33.6	3.6	25.8	40.7	29.4	2.0	24.8	33.0
Kreisbach be-sp	mixed	beech	32	68	4.2	50	73	68	4	50	73	35.9	9.1	15.4	54.4	29.8	3.1	20.9	33.8
	mixed	spruce	28	64	4.7	53	70	64	5	53	70	35.5	7.4	21.8	54.2	30.6	2.2	25.2	35.3
	pure	beech	30	72	5.8	46	82	72	6	46	82	32.1	6.0	18.9	43.6	31.8	1.8	26.4	35.0
	pure	spruce	30	61	4.8	48	71	61	5	48	71	42.9	8.3	28.4	62.3	31.7	1.9	27.6	34.3
Maissau 1 ok-pi	mixed	oak	29	55	13.0	41	81	56	13	41	81	22.6	8.9	9.4	38.4	19.2	3.9	8.4	25.1
	mixed	pine	31	49	3.6	34	54	49	4	34	54	21.4	3.1	10.9	29.6	19.8	2.0	13.6	23.2
	pure	oak	30	84	12.5	33	95	84	12	34	95	29.5	9.2	9.3	40.3	18.9	5.2	4.4	26.6
	pure	pine	30	42	6.5	31	57	66	7	56	84	22.1	4.1	12.9	29.5	20.4	1.9	14.5	24.7
Maissau 2 ok-pi	mixed	oak	29	87	15.0	67	111	87	15	67	111	28.2	10.1	9.4	48.0	18.7	4.7	5.8	24.9
	mixed	pine	30	103	15.4	78	130	103	15	78	130	28.1	9.7	8.4	47.1	19.1	4.6	9.6	26.1
	pure	oak	30	97	10.4	77	108	97	10	77	108	35.1	7.9	20.6	49.1	19.5	2.0	14.8	23.9
	pure	pine	31	122	11.8	79	148	122	12	79	148	27.2	4.3	18.8	36.2	20.3	2.4	13.2	23.9
Nassereith pi-sp	mixed	pine	32	122	3.4	108	127	122	3	108	127	47.5	5.6	35.8	58.3	30.6	3.5	22.8	37.0
	mixed	spruce	30	105	15.7	72	126	105	16	72	126	38.6	9.2	22.8	53.1	28.8	5.0	20.3	38.4
	pure	pine	30	58	3.0	51	64	58	3	51	64	28.1	4.8	15.4	36.1	19.3	1.7	15.0	22.8
	pure	spruce	31	104	7.6	83	120	104	8	83	120	32.0	6.5	23.4	49.2	25.5	3.8	17.7	33.3

$$\mathbf{R}_2 = \begin{pmatrix} 1 & -2 & 1 \\ 1 & -2 & 1 \\ & \ddots & \ddots & \ddots \\ & & 1 & -2 & 1 \end{pmatrix}$$

being a matrix reflecting the second-order neighborhood structure. In R-INLA, the precision parameter τ_2 was represented as $\theta_2 = \log(\tau_2)$, and a diffuse log-gamma prior was defined on θ_2 . Please note that only a single prior was required for the simultaneous smoothing of the approx. 30 tree-ring width series per sample plot.

Similar to Nothdurft and Vospernik (2018) and Nothdurft and Engel (2020), it was assumed that the effects of the monthly climate variables were inter-correlated. This was modeled with first-order random walks (RW1) for the coefficients γ_k , δ_k , and κ_k across the l lags and Gaussian i.i.d. assumptions for their increments between two consecutive lags

$$\nabla\gamma_k = \gamma_k - \gamma_{k-1} \sim N(0, \tau_3^{-1}),$$

$$\nabla\delta_k = \delta_k - \delta_{k-1} \sim N(0, \tau_4^{-1}),$$

$$\nabla\kappa_k = \kappa_k - \kappa_{k-1} \sim N(0, \tau_5^{-1}),$$

$$k = 2, \dots, l.$$

The density of the $l - 1$ increments followed a multivariate Gaussian distribution, and for example it was

$$\pi(\boldsymbol{\gamma} | \tau_3) \propto \tau_3^{(l-1)/2} \exp\left\{-\frac{1}{2}\boldsymbol{\gamma}^T \mathbf{Q}_3 \boldsymbol{\gamma}\right\}$$

in case of the γ_k coefficients. The precision matrix of γ , δ , and κ reads as $\mathbf{Q}_r = \tau_r \mathbf{R}_r$ with $r \in \{3, 4, 5\}$ where

$$\mathbf{R}_r = \begin{pmatrix} -1 & 1 & & & \\ & -1 & 1 & & \\ & & \ddots & \ddots & \\ & & & -1 & 1 \end{pmatrix} \quad \text{and} \quad \mathbf{R}_3 = \mathbf{R}_4 = \mathbf{R}_5$$

is the constant matrix reflecting the first-order neighborhood structure. Diffuse log-gamma priors were defined on the representations $\theta_3 = \log(\tau_3)$, $\theta_4 = \log(\tau_4)$, and $\theta_5 = \log(\tau_5)$ of the precision parameters τ_3 , τ_4 , and τ_5 .

By using the R-INLA defaults, the RW1 components were constrained to a sum-to-zero assumption. In this context, it was helpful to rescale the monthly climate measures. For this purpose, long-term monthly averages of both climate variables were calculated for the period 1971–2000. Consequently, the actual monthly temperatures were centered to the respective long-term monthly temperatures, and the monthly precipitation amounts were standardized by the respective long-term monthly precipitation values. Various candidate models were fitted that differed in their maximum number of lags l .

Because the sum-to-zero constraints were also applied to the RW2 smooths $f_i(\text{Age}_i)$, it was further necessary to introduce $\mathbf{u}_i \sim N(0, \tau_6^{-1})$, an independent Gaussian random intercept for each tree. Its precision parameter was represented as $\theta_6 = \log(\tau_6)$, for which a log-gamma prior was used. Finally, R-INLA internally added a tiny amount of extra noise ϵ_i to the linear predictor to avoid the situation where the joint distribution of η became singular.

Computations were performed in R (R Core Team, 2020) by using the R-INLA package (Lindgren and Rue, 2015). A short overview of the methodological fundamentals, further information on the program settings, and references to the seminal subject literature can be seen in the electronic supplementary material.

2.5. Excursion sets with uncertainty quantification for climate effects

Special effort was made for the quantification of uncertainty in the posterior estimates of the γ , δ , and κ parameters, which were modeled with RW1 priors across the l lags. The goal was to test at which of the l lags these parameters were different from zero. Vice versa, the interest lay in testing the null hypotheses

$$H_0^{(\gamma)}: \gamma_k = 0,$$

$$H_0^{(\delta)}: \delta_k = 0,$$

$$H_0^{(\kappa)}: \kappa_k = 0,$$

$$\forall k \in \{1, \dots, l\},$$

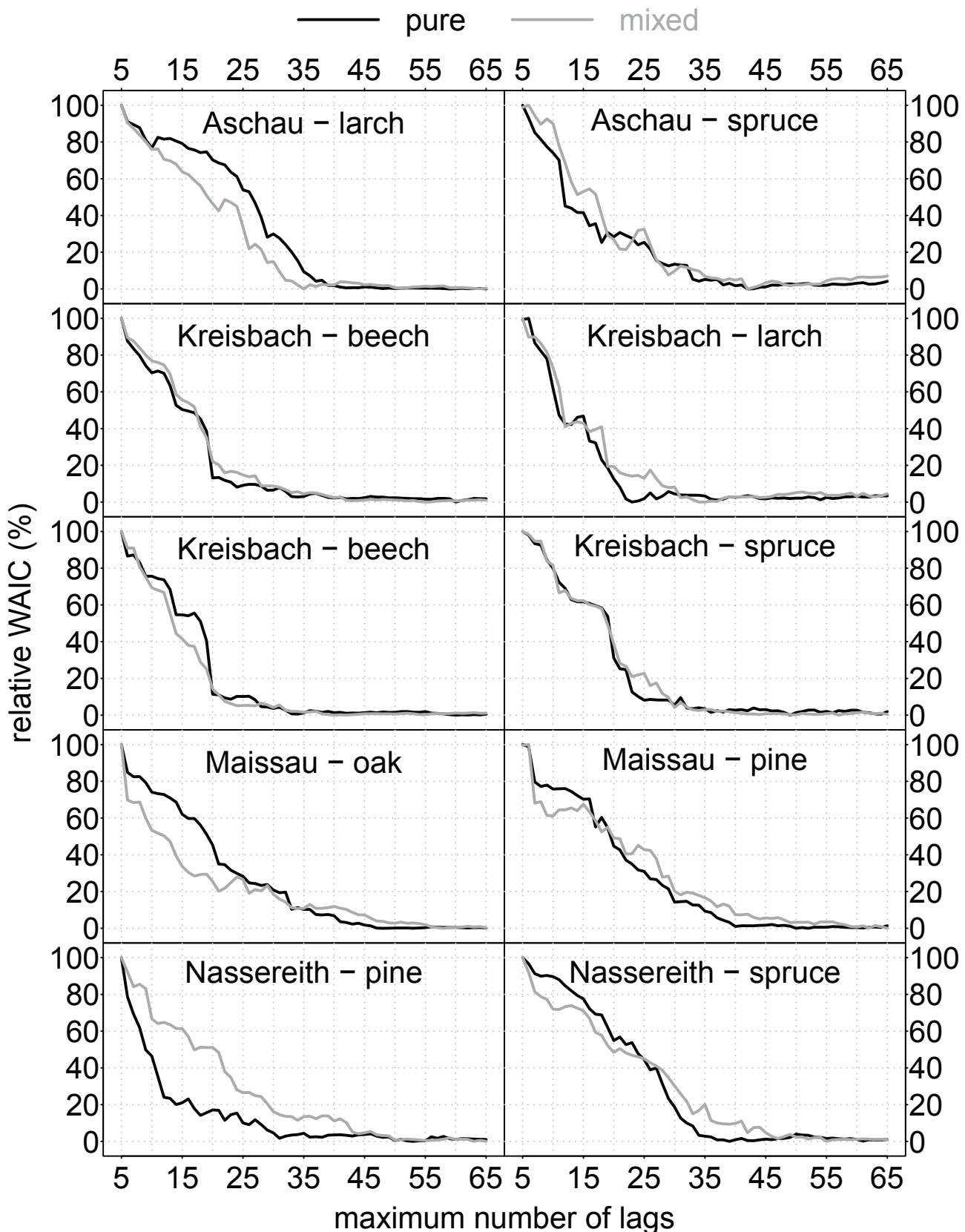


Fig. 2. WAIC of candidate models with different numbers of maximum lags in the climate-sensitive distributed lag model terms. Per each site, species, and mixture type, the absolute WAIC values were transformed to the percentage scale. That is, the model with the maximum WAIC represented 100%, and the model with the lowest WAIC represented 0%.

stating that all parameters across the entire set of lags had zero values throughout. In fact, if these tests would have been performed sequentially, a total number of l tests for each of the three aforementioned parameters would have been necessary. Thus, analogous to the frequentist perspective, a multiple testing problem was present. That made it necessary to consider a “family-wise” α -error rate, which quantified the uncertainty of the corresponding H_1 -assumptions that the parameters were actually different from zero.

To perform such tests for the parameters of the climate-sensitive distributed lag model, I used the methods that were implemented in the R package `brinla` (Faraway et al., 2020). The computations in `brinla` work on the latent Gaussian field and use parametric assumptions for the excursion sets in combination with sequential importance sampling for the joint probabilities; see Bolin and Lindgren (2015) for further details. The `brinla` package offers five different methods for the handling of the latent Gaussian structure, of which I used the “numerical integration with quantile correction” method (NIQC).

2.6. Prognoses with Bayesian predictive functions

To examine whether a long-term climate related growth trend existed, Bayesian predictions were made with a posterior predictive function. In this predictive function, only a subset of the linear predictor (Eq. 1) was used that comprised the three climate-sensitive terms of the distributed lag model, but that omitted the RW2 smooth component $f_i(\text{Age}_i)$ and the tree-level zero-mean Gaussian offset \mathbf{u}_i . Predictions with R-INLA do not need a posterior predictive simulation, such as with traditional MCMC-based approaches. They were achieved as part of the model fitting itself instead.

Posterior uncertainty of the long-term climate-related predictions was assessed by using the highest posterior density (HPD) intervals. A HPD interval spans the region of values that contains $100(1 - \alpha)\%$ of the posterior probability. Simultaneously, the density within that region is never lower than outside. Consequently, the HPD interval is the shortest among all possible $100(1 - \alpha)\%$ intervals and represents the collection of most likely parameter values; for further details on HPD intervals, the reader is referred to standard textbooks on Bayesian data analysis, e.g., Gelman et al. (2004).

Post-hoc linear models were used to assess whether climate-related long-term growth trends existed, and to compare whether the possible trends differed between both the pure- and mixed-stand scenario. Post-hoc F-tests were used to examine whether the climate-related fluctuations of the Bayesian predictions in summary showed wider oscillations under the pure-stand scenario than under the mixed-stand scenario.

3. Results

3.1. Maximum number of lags

For each tree species and mixture type per site, candidate models were fitted that differed in their maximum number of lags l of the climate sensitive terms in the linear predictor (Eq. 1). More precisely, models were tested that had a maximum number of lags corresponding to all integers within the sequence from 5 to 65 lags. According to the recommendation in Gelman et al. (2014), I preferred the Watanabe Akaike information criterion (WAIC) (Watanabe, 2010) against the deviance information criterion (DIC) (Spiegelhalter et al., 2002) when I compared the performance of the different models.

To achieve a clear presentation and an easy comparison, the WAICs of the models were transformed to the percentage scale. In so doing, the model with the lowest absolute WAIC represented a relative WAIC of 0% and the model with the highest absolute WAIC had a relative WAIC of 100% (Fig. 2). It became obvious that the WAIC sharply decreased with an increasing number of considered lags. However, under further model extensions beyond approximately 36 lags, the decreases in WAIC became relatively small, and the WAIC reached nearly a steady level.

Such behavior was similar across all sites, species, and mixture types. Thus, the decrease occurred equally rapidly for any of the examined species or mixture types. In consequence, final models were re-fitted having a constant maximum number of $l = 36$ lags and by using the simplified Laplace approximation strategy, instead of a Gaussian approximation. That means, throughout all sites, species, and mixture types, monthly climate measures were considered at earliest for October three years prior to the current season, in which a tree-ring was built. Inference on the posterior of the hyperparameters and the latent field was only derived from these final models having $l = 36$.

3.2. Hyperparameters

Summary statistics of the posterior densities for the gamma dispersion parameter ϕ and the precision parameters $\tau_2 - \tau_6$ are reported in Tables S1–S3 in the electronic supplementary material. This information could also guide others in their choices of appropriate priors.

Whereas, τ_6 was a tree-level offset random parameter and accounted for the inter-tree variance among the tree-ring width times series, τ_2 determined the roughness of the RW2 smooths and represented the intra-tree variance of the series. In 13 out of a total of 20 cases (models), the posterior mean of precision parameter τ_6 was higher than the posterior mean of precision parameter τ_2 . That means the within-tree increment variance (τ_2^{-1}) was in most cases higher than the between-tree intercept variance (τ_6^{-1}).

In the climate-sensitive distributed model terms, τ_3 determined the precision of the RW1 smooth for the time-lagged temperature effects, τ_4 determined that for the precipitation effects, and τ_5 determined that for the interaction between both monthly climate measures. In all cases, the posterior mean of the precision parameter τ_3 was higher than the posterior mean of τ_4 . From this it follows that the effects of deviations from long-term monthly average temperatures had a lower variance across the lags than the time-lagged precipitation effects. In 7 out of 20 cases, the posterior mean of the precision parameter τ_5 was higher than the posterior mean of τ_3 , which means that in most cases the RW1 smooth for the time-lagged effects of temperature deviations reflected a higher variance than that for the climate interaction effects. Evidence was lacking that this happened more frequently at lower or higher elevation sites, or for coniferous or deciduous tree species, or in pure or mixed stands.

3.3. Detrending

It was examined whether the detrending with $f_i(\text{Age}_i)$ was not too wiggly on the one hand but flexible enough to consider medium-term oscillations on the other hand. For this purpose, the posterior mean and 95% credible intervals were derived from the marginal predictive distribution based on a subset linear predictor that contained only the tree-level offset \mathbf{u}_i and the RW2 smooth component $f_i(\text{Age}_i)$. Comparisons of the smooths with the observations (see Figs. S1–S24 in the electronic supplementary material) showed that the flexibility of the former was appropriate throughout.

3.4. Climate effects

The posterior estimates of the effects of the monthly climate variables considered by the distributed lag model terms were presented in Fig. 3. The posterior mean of the climate effects was indicated by line plots across the lag sequence. When reading the plots from left to right, the lines start at the first lag ($l = 1$) for the most recent month, and they end at the last lag ($l = 36$) for the earliest month in the past. Credible intervals and family-wise hypothesis tests for excursion sets were used to evaluate the significance of the effects of monthly climate variables in the distributed lag model terms.

Larch in Aschau. Higher temperatures in the current year's early summer and spring had positive effects. Warm temperatures during the

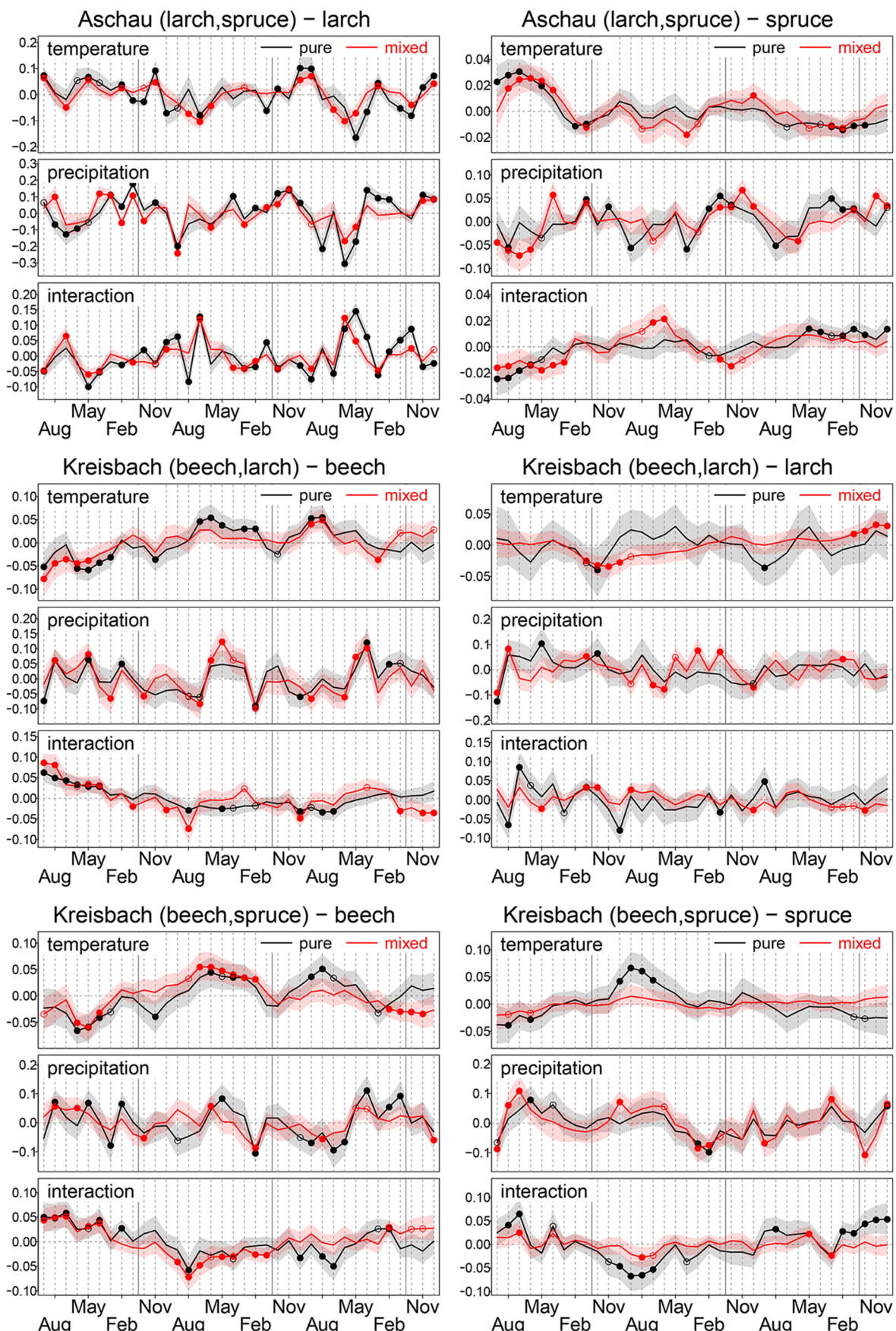


Fig. 3. Effect curves (posterior mean) for the monthly climate variables modeled with first-order random walk priors across the lags (solid lines), 90% credible intervals (shaded areas), and significant effects under family-wise $\alpha = 0.05$ (solid circles) and $\alpha = 0.1$ (empty circles) error rates.

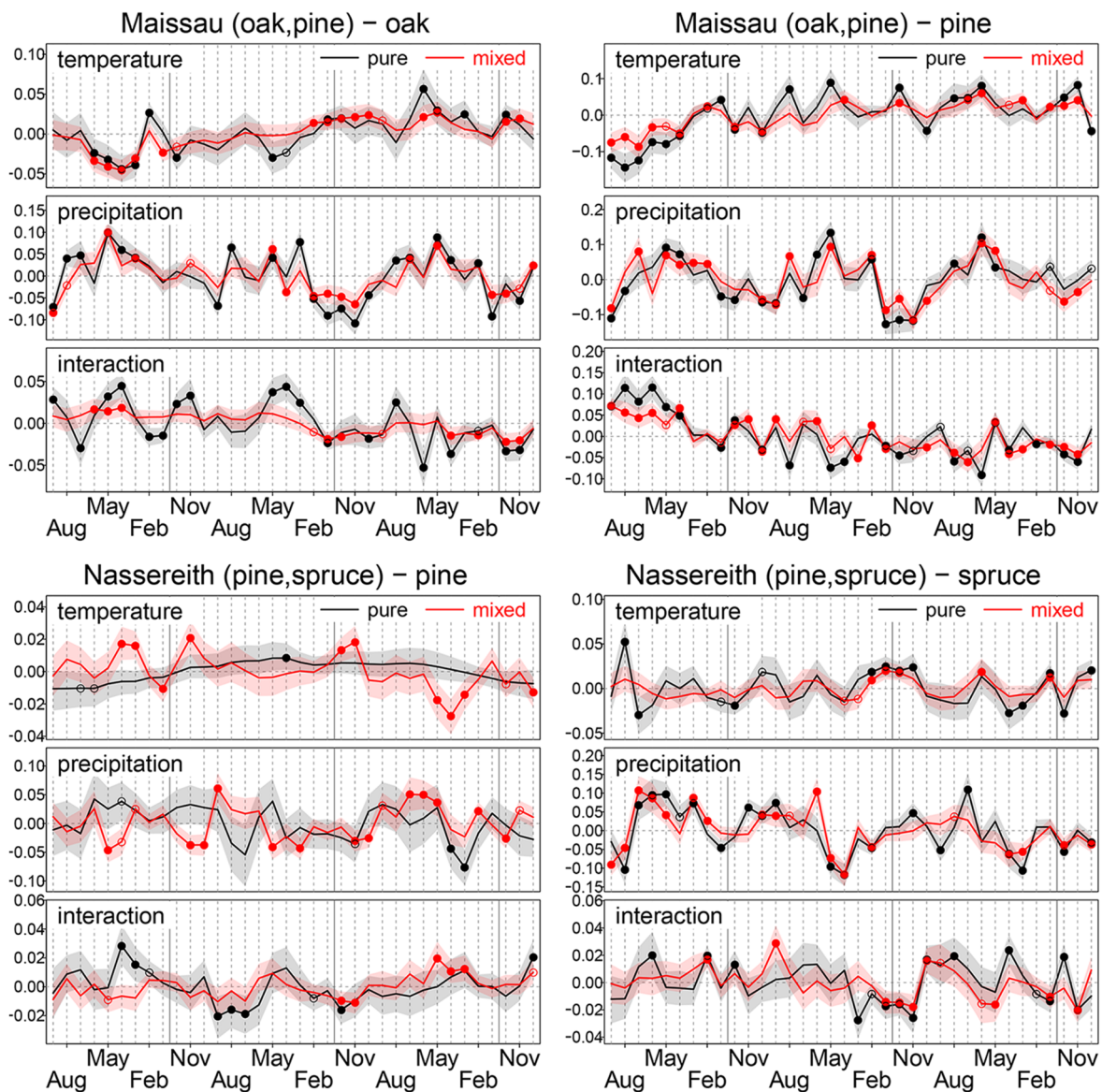


Fig. 3. (continued)

late summer and autumn of the preceding year had negative effects. Two years back, warm autumn temperatures were favorable, but a warm summer was unfavorable. Meanwhile, higher precipitation during the current as well as the past growing seasons had negative effects, and higher precipitation during the springs and winters was positive. The interaction effect of higher temperature and higher precipitation was negative for the summer, but it was positive for the last autumn. Monthly climate measures during the spring two years ago had a positive interaction effect. The patterns of the climate effects were similar under the pure and mixed scenario, but their magnitude was slightly stronger under the former.

Spruce in Aschau. Higher temperatures during the current growing season had positive effects throughout, but higher summer temperatures in the past growing seasons had negative effects. Such as for larch, higher precipitation during the current as well as the past growing seasons was unfavorable, but higher precipitation during the current as well as the past spring and winter periods had positive effects. The interaction effect of high temperature and precipitation in the current growing season was negative, and it was positive for the past growing seasons. The climate effects were similar between both mixture scenarios, but they were slightly stronger in the pure stand.

Beech in Kreisbach (beech-larch triplet). Higher temperatures in the current growing season had negative effects throughout. A warm spring and warm summer in the preceding year as well as a warm late summer two years back had positive effects. Higher precipitation during the spring in the preceding year and two years before were favorable. A strong positive interaction effect existed between warmer temperatures and higher precipitation for the current growing season. That means, a hot and dry climate during the current growing season was unfavorable, but hot temperatures associated with high precipitation provided favorable growth conditions. The climate effects were similar under both mixture scenarios, but they were stronger in the pure stands.

Larch in Kreisbach (beech-larch triplet). A warm winter temperature was counterproductive. However, the effects of the other average monthly temperatures were undifferentiated. The role of precipitation was also less relevant. A slightly positive interaction existed between warmer temperatures and higher precipitation amounts in the current early summer. The temperature effects were more clear under the mixed-stand scenario, but the interaction effects were more relevant in the pure stand.

Beech in Kreisbach (beech-spruce triplet). All three RW1 climate effect curves for the beech trees from the beech-spruce triplet plots were similar to those from the beech-larch triplet plots.

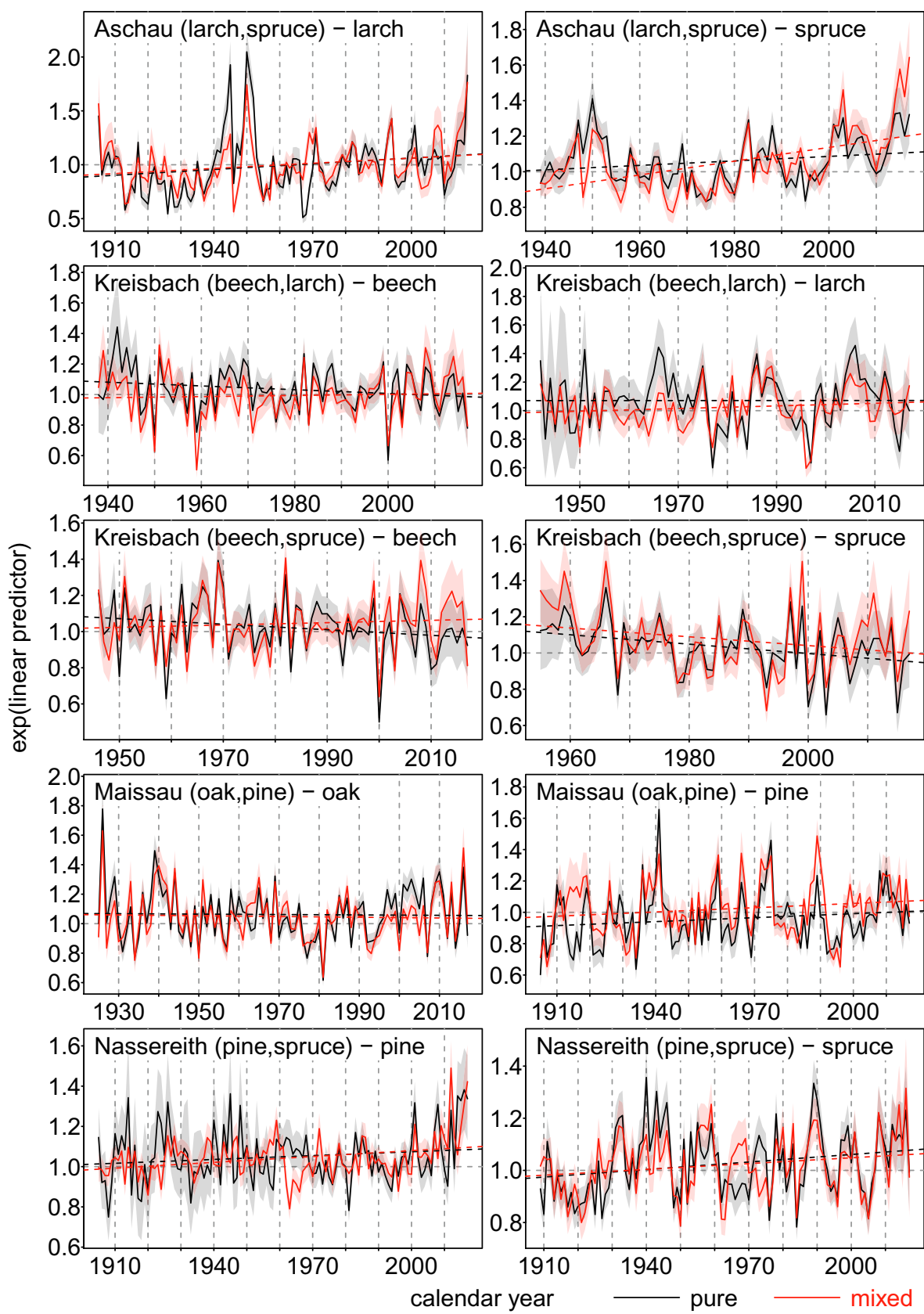


Fig. 4. Bayesian predictions and 95% highest posterior density intervals for past climate-sequences achieved with the distributed lag model terms of the linear predictor. Post-hoc linear models for long-term growth trends (dashed lines).

Spruce in Kreisbach (beech–spruce triplet). High temperatures during the current growing season had negative effects, but those of the preceding growing season had positive effects. While higher precipitation in the current as well as the preceding growing season was favorable, higher late winter precipitation, especially of the preceding year, was unfavorable. Warm temperatures and high precipitations had positive interaction effects during the current growing season and negative effects during the summer months of the preceding season. The temperature as well as interaction effects were less significant under the mixed-stand scenario.

Oak in Maissau. Warm temperatures in the current year's late spring and early summer had negative effects. Under the pure-stand scenario, warm spring temperatures during the preceding growing season likewise had negative effects. Warmer winter temperatures two years back had positive effects. Higher precipitation during the growing seasons was always favorable, but higher precipitation during the winter two years ago had negative effects. A positive interaction existed between higher temperatures and precipitation during the current and the preceding spring; this was especially observed for the pure-stand scenario. That means, a hot climate during the growing season was favorable if precipitation was high; otherwise hot temperatures were unfavorable.

Pine in Maissau. A hot climate in the current growing season had strong negative effects, such as the mild mid-winter temperatures had. However, warmer summer temperatures two years back had positive effects. Higher precipitation was beneficial during a longer period in the current year reaching from February until the end of summer, and likewise for last year's early spring and mid-summer, and for the mid-summer two years ago. Higher precipitation had negative effects during the preceding autumn and the mid-winter periods of the last two years. Temperature and precipitation showed strong positive interaction effects during the current year's growing season. Hence, a hot and dry climate during the current growing season was counterproductive, but warmer temperatures in conjunction with a higher precipitation were beneficial. In summary, climate effects were stronger under the pure than the mixed-stand scenario.

Pine in Nassereith. In the pure stand, temperature effects were mostly insignificant, but in the mixed stand warmer spring temperatures had positive effects. Higher precipitation had positive effects during the summer two years ago, and in the same year's spring it was unfavorable in the mixed stand. Interaction effects were less relevant for the mixed stand. A warm and humid climate in spring was favorable for the pure stand, but it was unfavorable during the preceding growing season.

Spruce in Nassereith. Higher winter temperatures during the last winter had negative effects, but these had positive effects two years ago. Higher precipitation during the current and the preceding growing season increased the single tree productivity rates. However, higher precipitation during the early spring of the last two years had negative effects. Higher temperatures and precipitation showed strong negative interaction effects for the winter time two years ago. Stronger positive interaction effects occurred during late summer two years ago. The climate effects under the pure-stand scenario were stronger throughout than under the mixed-stand scenario.

3.5. Prognoses with predictive functions

Bayesian predictions were made with posterior predictive functions to evaluate the climate-related long-term growth trends on the sample plots (Fig. 4). Summary statistics of the post hoc trend analysis with linear models and the diagnostics of the variance tests are reported in Table S4.

For the larch trees in Aschau, the annual increment rates showed equally strong positive trends in both the pure and mixed-stand scenario. The post hoc variance test revealed that single-tree productivity rates under the mixed-stand scenario had a lower climate-related

sensitivity than that under the pure-stand scenario. The increment rates of spruce likewise showed a positive trend, with a steeper increase in the mixed-stand. The climate-related oscillations were wider in the pure spruce stand.

On the beech–larch triplet plots, productivity of beech showed a slightly negative trend in the pure stand and a neutral trend (i.e., neither positive or negative) in the mixed stand. The climate-related oscillation was equally high under both mixture scenarios. The increments of larch did not show a significant trend, neither in the pure nor in the mixed stand. Climate-sensitivity of the larch increments was significantly lower in the mixed stand.

On the beech–spruce triplet plots, productivity of beech had trends that were similar to the beech–larch triplet, slightly negative in the pure stand and neutral in the mixed stand. Climate-related oscillations of the Bayesian predictions were almost equally high under both mixture scenarios. Productivity of spruce on the beech–spruce triplet plots in Kreisbach had an equally strong negative trend in the pure and mixed stands. Climate-sensitivity was higher in the mixed stand.

Productivity of oak did not show a significant long-term climate-related trend in Maissau, neither under the pure nor the mixed scenario. The climate-related oscillations were likewise similar under both scenarios. In contrast, productivity of the pine trees had a weak positive trend under both scenarios. The climate-related oscillations of the pine trees were similar under both mixture scenarios.

Such as in Aschau, the pine trees also showed a positive long-term growth trend in both stands at the other Tyrolean site in Nassereith. The climate-related oscillations of the pine trees were significantly lower under the mixed-stand scenario. The productivity of the spruce trees in Nassereith also had a positive trend under both scenarios, and climate-sensitivity was likewise reduced by the species mixture.

3.6. Key model results

At the low elevation sites Kreisbach and Maissau, the annual radial stem increment of beech, oak, pine, and spruce was generally reduced by warmer temperatures during the current growing season. In contrast, the productivity of larch was relatively resistant against hot summer temperatures. At these low elevation sites, higher precipitation during the current growing was always favorable, and higher precipitations during the past growing seasons additionally had positive time-lagged effects. A hot and dry climate had a negative effect, in general. However, if warmer temperatures were associated with high precipitation the effect became clearly positive. The climate effects showed similar trends under both the pure- and mixed-stand scenario, but they were milder under the latter scenario.

At both Alpine sites Aschau and Nassereith, warmer temperatures during the growing season had positive effects. These effects were stronger in Aschau than in Nassereith, as the elevation in Aschau was higher and the average climate was colder. The increment rates of larch also showed positive reactions to warmer temperatures during the growing season, but these were weaker than the reactions of spruce. Temperature was less relevant for pine in Nassereith. While the winter precipitation had positive effects for larch and spruce in Aschau, the precipitation during the growing seasons was more relevant for pine and spruce in Nassereith. These respective precipitation patterns also had strong positive time-lagged effects. The interaction between a higher temperature and higher precipitation during the past growing season was generally positive on both sites. However, the interaction effect was negative during the preceding year for the pine trees in Nassereith, and it was also negative during the current growing season for spruce in Aschau.

The coniferous tree species larch, pine, and spruce showed positive trends at the high elevation sites in Aschau and Nassereith, irrespective of the pure/mixed-stand scenario. In addition, the presence of a species mixture lowered the climate-related increment oscillations of larch and pine at these sites. At the lower elevation sites in Kreisbach, spruce

showed severe negative growth trends under both scenarios, and beech showed only a (milder) negative growth trend in the pure stand. While the productivity of oak and larch remained constant on the lower elevation sites in Maissau and Kreisbach, pine may have even benefited from the climate changes in the past. The latter trends remained nearly unaffected by a mixture situation. At the lower elevation sites, the presence of a species mixture reduced the climate-related increment oscillations of larch and enhanced the oscillations of spruce. The climate-sensitivity of beech and pine was not influenced by a species mixture on these sites.

3.7. Diagnostics of the Bayesian predictions and residuals

Line plots for the time-series of the Bayesian predictions and the observations per tree showed that the Bayesian hierarchical models provided a good fit to the data throughout; see Figs. S25–S48 in the electronic supplementary material. The models were obviously able to represent the medium-term oscillations considered by the RW2 smooths as well as the short-term fluctuations modeled with the climate-sensitive distributed lag model. Scatter plots of the Bayesian predictions versus the observations (Fig. S49 in the electronic supplementary material) showed that the points were independently and closely distributed around the reference lines with zero intercepts and slopes of one. In summary, the models were regarded as well specified and provided proper fits to the data.

4. Discussion

4.1. Empirical findings

The detected climate effects at higher elevation sites were similar to those reported in Nothdurft and Vospernik (2018), in that growth at these sites is constrained by thermal limitations during the growing season (Körner, 1998), and in that winter precipitation in the form of snowfall is relevant (Oberhuber, 2004) as it builds a snow pack that serves as a water reservoir and functions as a protection layer. Such as formerly presented in Nothdurft and Vospernik (2018), I also observed a positive long-term growth trend at these higher elevation sites. By using other data, I could confirm this trend especially for spruce, and I could show that this trend is also present for larch and pine. It is a novel finding that these trends obviously remain unaffected by a mixture scenario.

By using a different inferential framework, I could confirm the findings in Nothdurft and Engel (2020) for the lower elevation sites, in that hot temperatures during the current growing season lower the productivity, and in that precipitation during the growing season is rather favorable. However, larch trees obviously behave differently. The increment rates of spruce particularly show a strong negative climate-related growth trend, which is not changed by the admixture of beech. This seems contrary to the findings in Pretzsch et al. (2014) of a general positive growth trend throughout Central European forest ecosystems. However, I assume that hidden climate-related increment losses (Hartl-Meier et al., 2014) could have already existed in the past but they were so far overcompensated by a higher nitrogen supply (Braun et al., 2017).

For the lower elevation sites, I also found that beech showed a negative growth trend in the pure stand, but in coexistence with spruce or larch, the trend diminished. This is certainly because the strong competitive intra-species stress of beech is reduced through the admixture of other tree species (Pretzsch et al., 2010) and is especially evoked by modified crown allometries (Dieler and Pretzsch, 2013; Pretzsch, 2014).

Simultaneously, I could not find negative growth trends for larch and oak on the lower elevation sample plots, and even a positive trend was observed for pine. Furthermore, none of these latter phenomena were obviously changed by a mixture scenario. The high drought-stress tolerance of oak mainly results from manifold ecophysiological mechanisms, among them a sustained stomatal conductance under low water potentials (Bahari et al., 1985), a fine-root biomass productivity that is insensitive to

drought (Leuschner et al., 2001), and dynamic adaptations through a reduction of leaf/root ratios and via the production of second flushes and buds (Thomas, 2000). The distinct drought tolerance of pine relies on the wax-lined epidermis structure and the enhanced stomata control of the needles (Krakau et al., 2013). Because of the aforementioned physiological characteristics and the empirical evidence for their stationary growth patterns, oak and pine are broadly termed as being well-adapted to future climate changes that will be very likely associated with an increased severity and a longer duration of drought periods. Furthermore, the mixture of both species of oak and pine obviously does not change their suitability, because complementary effects occur through reduced competition and facilitation (Ammer, 2019). The constant productivity rates of larch are likewise manifested by a high resistance against dehydration, which has been confirmed in experiments (Plesa et al., 2018). The high water-use efficiency of larch has an epigenetic foundation (Zhang and Marshall, 1994), which also determines memory (carry-over) effects in terms of an invariable spring phenology (Gömöry et al., 2015).

In conformance with prior results in Nothdurft and Engel (2020), I found that the mixture can reduce climate-related increment fluctuations (Pretzsch et al., 2013; Metz et al., 2016), but not for beech, spruce, oak, and pine growing at lower elevation sites. Even higher increment fluctuations in mixed oak-pine stands were indicated by others (Merlin et al., 2015; Toigo et al., 2015; Bonal et al., 2017), and higher increment oscillations of spruce in mixed stands were formerly suggested in Dănescu et al. (2018).

4.2. Methodology

Thus far, hierarchical Bayes models have been also introduced to dendrochronological analyses in other studies (Foster et al., 2016; Iter et al., 2017; Iter et al., 2019). However, the utilization of INLA is novel. The construction of the hierarchical Bayes models with R-INLA was straightforward. A sparse model formulation was achieved that required only a total number of six hyperparameters. The novel Bayesian framework provides a sound technique for uncertainty assessment from the marginal posteriors, including credible intervals, HPD intervals, and family-wise hypothesis tests on excursion sets. The computations with R-INLA were fast and required, on average and per model, 30 min with the simplified Laplace approximations and only 4 min with the Gaussian approximations when using a modern standard desktop computer.

In my hierarchical Bayesian approach, the climate sensitive terms of the distributed lag model were formulated as a linear model. This was much simpler but also less flexible than in my formerly applied GAM approaches (Nothdurft and Vospernik, 2018; Nothdurft and Engel, 2020) that were based on penalized regression splines. In fact, I also made some trials with B-spline basis functions and two-dimensional random-walk priors in R-INLA. However, model fitting became computationally demanding, prediction was no longer straightforward, and the effect curves were often implausible.

The simultaneous modeling of the ring-width increments from both the pure and the mixed stand data was tested. The idea was to consider the differences in the distributed lag models by extra priors for random walks that should have acted as offset terms. However, such simultaneous modeling was computationally not feasible.

Another initial idea was to use the Bayesian model framework for the explicit exploration of an optimum number of lags. However, the number of effective parameters, which is used as penalty in the WAIC to adjust for overfitting, did not change much for different l , the maximum number of lags. Hence, the WAIC curves in Fig. 2 showed a continuously declining trend, and the choice of a constant l for all models was guided rather by heuristics than by a statistical hypothesis test.

5. Conclusions

In summary, I was able to verify my initially formulated hypothesis, in that climate-related growth trends at lower and higher elevation sites

generally had opposite signs, with clear positive trends at the high elevation sites. Furthermore, the climate-related productivity rates of the drought tolerant species larch, oak, and pine actually behaved stationary at the lower elevation sites, such as was initially expected. I must generally reject my hypothesis that a mixed-species neighborhood weakens the growth trends, as this occurred only for the growth trend of beech at the lower elevation sites. Finally, evidence is lacking that species mixing generally lowers the climate-related increment fluctuations. In fact, species mixing did not change the increment fluctuations of beech, oak, and pine, and it even increased those of spruce at lower elevation sites, in particular.

Consequently, oak, pine, and larch can be considered as well adapted to future climate changes on lower elevation sites in Austria. These tree species will certainly provide an unchanged productivity level under such circumstances. However, severe increment losses are rather expected for spruce at the lower elevation sites, and cultivation in mixed-stands with beech will not hinder the expected productivity decreases of spruce. The admixture of beech is even unfavorable for spruce and would increase the climate-related increment fluctuations of the latter tree species.

Vice versa and as seen from a different perspective, the cultivation of spruce as an admixture to beech could have positive effects because it will buffer the productivity losses, which would otherwise occur in pure beech stands. Hence, the cultivation of mixed beech-spruce stands is recommended in place of pure beech or pure spruce stands, but significant benefits can be expected only for the beech trees. The admixture of larch to beech stands would have a similar effect. However, silvicultural management of mixed beech-larch stands is more complicated than the management of mixed beech-spruce stands is, as both species of the former mixture type have a completely different light demand. Spruce, larch, and pine will certainly show further increased productivity levels in future periods on alpine sites, and the expected gains will not be changed when these species are cultivated in a joint mixture type.

Thanks to R-INLA, the implementation of the hierarchical Bayes models is straightforward and these models can be easily used to build modern statistical forest growth models. The novel methodology offers versatile techniques for uncertainty assessments that can be also applied to complex model formulations and to challenging test problems in the context of other climate change impact studies.

Declaration of Competing Interest

None.

Declaration of Competing Interest

The authors declare that they have no known competing financial interests or personal relationships that could have appeared to influence the work reported in this paper.

Acknowledgments

This study was supported by the project REFORM under the umbrella of the ERA-NET project Sumforest and was locally financed by the Austrian Federal Ministry of Agriculture, Regions and Tourism under project number 101199. I am particularly grateful to Dr. Heidi Bäuerle for fruitful and inspiring discussions of the applicability of INLA in a forestry context. I appreciate very much the constructive and helpful comments given by the two anonymous reviewers.

Appendix A. Supplementary material

Supplementary data associated with this article can be found, in the online version, at <https://doi.org/10.1016/j.foreco.2020.118497>.

References

- Ammer, C., 2019. Diversity and forest productivity in a changing climate. *New Phytol.* 221, 50–66.
- Anderegg, L.D., HilleRisLambers, J., 2016. Drought stress limits the geographic ranges of two tree species via different physiological mechanisms. *Glob. Change Biol.* 22 (3), 1029–1045.
- Bahari, Z.A., Pallardy, S.G., Parker, W.C., 1985. Photosynthesis, water relations, and drought adaptation in six woody species of oak-hickory forests in central Missouri. *Forest Sci.* 31 (3), 557–569.
- Beniston, M., Stephenson, D.B., Christensen, O.B., Ferro, C.A., Frei, C., Goyette, S., Halsnaes, K., Holt, T., Jylhä, K., Koffi, B., Palutikof, J., 2007. Future extreme events in European climate: an exploration of regional climate model projections. *Clim. Change* 81 (1), 71–95.
- Bolin, D., Lindgren, F., 2015. Excursion and contour uncertainty regions for latent Gaussian models. *J. Royal Stat. Soc. Series B (Stat. Methodol.)* 77 (1), 85–106.
- Böhm, R., Auer, I., Schöner, W., Ganeck, M., Gruber, C., Jurkovic, A., Orlik, A., Ungerböck, M., 2009. Eine neue Webseite mit instrumentellen Qualitäts-Klimadaten für den Grossraum Alpen zurück bis 1760. *Wiener Mitteilungen* 216, 7–20 http://www.hydro.tuwien.ac.at/uploads/media/Band_216-Teil-1_01.pdf.
- Bonal, D., Pau, M., Toigo, M., Granier, A., Perot, T., 2017. Mixing oak and pine trees does not improve the functional response to severe drought in central French forests. *Annals Forest Sci.* 74, 72.
- Braun, S., Schindler, C., Rihm, B., 2017. Growth trends of beech and Norway spruce in Switzerland: The role of nitrogen deposition, ozone, mineral nutrition and climate. *Sci. Total Environ.* 599–600, 637–646.
- Bréda, N., Badeau, V., 2008. Forest tree responses to extreme drought and some biotic events: Towards a selection according to hazard tolerance? *C.R. Geosci.* 340 (9–10), 651–662.
- Bréda, N., Huc, R., Granier, A., Dreyer, E., 2006. Temperate forest trees and stands under severe drought: a review of ecophysiological responses, adaptation processes and long-term consequences. *Annals Forest Sci.* 63 (6), 625–644.
- Castagneri, D., Battipaglia, G., von Arx, G., Pacheco, A., Carrer, M., 2018. Tree-ring anatomy and carbon isotope ratio show both direct and legacy effects of climate on bimodal xylem formation in *Pinus pinea*. *Tree Physiol.* 38 (8), 1098–1109.
- Dănescu, A., Kohnle, U., Bauhus, J., Sohn, J., Albrecht, A.T., 2018. Stability of tree increment in relation to episodic drought in uneven-structured, mixed stands in southwestern Germany. *For. Ecol. Manage.* 415–416, 148–159.
- Dieler, J., Pretzsch, H., 2013. Morphological plasticity of European beech (*Fagus sylvatica* L.) in pure and mixed-species stands. *For. Ecol. Manage.* 295, 97–108.
- Faraway, J., Yue, R., Wang, X., 2020. brinla: Bayesian Regression with INLA. R package version 0.1.0. <http://github.com/julianfaraway/brinla>.
- Foster, J.R., Finley, A.O., D'Amato, A.W., Bradford, J.B., Banerjee, S., 2016. Predicting tree biomass growth in the temperate-boreal ecotone: Is tree size, age, competition, or climate response most important? *Glob. Change Biol.* 22, 2138–2151.
- Fritts, H.C., 1976. Tree rings and climate. Academic Press, London, UK.
- Gelfand, A.E., Smith, A.F., 1990. Sampling-based approaches to calculating marginal densities. *J. Am. Stat. Assoc.* 85 (410), 398–409.
- Gelman, A., Carlin, J.B., Stern, H.S., Rubin, D.B., 2004. Bayesian Data Analysis. CRC Press.
- Gelman, A., Hwang, J., Vehtari, A., 2014. Understanding predictive information criteria for Bayesian models. *Stat. Comput.* 24 (6), 997–1016.
- Gobiet, A., Kotlarski, S., Beniston, M., Heinrich, G., Rajczak, J., Stoffel, M., 2014. 21st century climate change in the European Alps – a review. *Sci. Total Environ.* 493, 1138–1151.
- Gömöry, D., Foffová, E., Longauer, R., Krajmerová, D., 2015. Memory effects associated with early-growth environment in Norway spruce and European larch. *Eur. J. Forest Res.* 134, 89–97.
- Hartl-Meier, C., Zang, C., Büntgen, U., Esper, J., Rothe, A., Göttlein, A., Dirnböck, T., Treydte, K., 2014. Uniform climate sensitivity in tree-ring stable isotopes across species and sites in a mid-latitude temperate forest. *Tree Physiol.* 35 (1), 4–15.
- Hastings, W.K., 1970. Monte Carlo sampling methods using Markov chains and their applications. *Biometrika* 57 (1), 97–109.
- Itter, M.S., D'Orangeville, L., Dawson, A., Kneeshaw, D., Duchesne, L., Finley, A.O., 2019. Boreal tree growth exhibits decadal-scale ecological memory to drought and insect defoliation, but no negative response to their interaction. *J. Ecol.* 107, 1288–1301.
- Itter, M.S., Finley, A.O., D'Amato, A.W., Foster, J.R., Bradford, J.B., 2017. Variable effects of climate on forest growth in relation to climate extremes, disturbance, and forest dynamics. *Ecol. Appl.* 27, 1082–1095.
- Jacob, D., Petersen, J., Eggert, B., et al., 2014. EURO-CORDEX: new high-resolution climate change projections for European impact research. *Reg. Environ. Change* 14 (2), 563–578.
- Kannenberg, S.A., Novick, K.A., Alexander, M.R., Maxwell, J.T., Moore, D.J., Phillips, R.P., Anderegg, W.R., 2019. Linking drought legacy effects across scales: From leaves to tree rings to ecosystems. *Glob. Change Biol.* 25 (9), 2978–2992.
- Körner, C., 1998. A re-assessment of high elevation treeline positions and their explanation. *Oecologia* 115, 445–459.
- Krakau, U.K., Liesebach, M., Aronen, T., Lelu-Walter, M.A., Schneck, V., 2013. Scots pine (*Pinus sylvestris* L.). In: Paques, L.E. (Ed.), Forest tree breeding in Europe. Current State-of-the-art and Perspectives. Springer, Dordrecht, New York.
- Leuschner, C., Backes, K., Hertel, D., Schipka, F., Schmitt, U., Terborg, O., Runge, M., 2001. Drought responses at leaf, stem and fine root levels of competitive *Fagus sylvatica* L. and *Quercus petraea* (Matt.) Liebl. trees in dry and wet years. *For. Ecol. Manage.* 149 (1–3), 33–46.
- Leuzinger, S., Zott, G., Asshoff, R., Körner, C., 2005. Responses of deciduous forest trees

- to severe drought in Central Europe. *Tree Physiol.* 25 (6), 641–650.
- Lindgren, F., Rue, H., 2015. Bayesian Spatial Modelling with R-INLA. *J. Stat. Softw.* 63 (19), 1–25.
- van der Maaten-Theunissen, M., Bümmertede, H., Iwanowski, J., Scharnweber, T., Wilmking, M., van der Maaten, E., 2016. Drought sensitivity of beech on a shallow chalk soil in northeastern Germany — a comparative study. *Forest Ecosyst.* 3, 24.
- Martins, T.G., Simpson, D., Lindgren, F., Rue, H., 2013. Bayesian computing with INLA: New features. *Comput. Stat. Data Anal.* 67, 68–83.
- Merlin, M., Perot, T., Perret, S., Korboulewsky, N., Valler, P., 2015. Effects of stand composition and tree size on resistance and resilience to drought in sessile oak and Scots pine. *For. Ecol. Manage.* 339, 22–33.
- Metropolis, N., Rosenbluth, A.W., Rosenbluth, M.N., Teller, A.H., Teller, E., 1953. Equation of state calculations by fast computing machines. *J. Chem. Phys.* 21 (6), 1087–1092.
- Metz, J., Annighöfer, P., Schall, P., Zimmermann, J., Kahl, T., Schulze, E.-D., Ammer, C., 2016. Site-adapted admixed tree species reduce drought susceptibility of mature European beech. *Glob. Change Biol.* 22 (2), 903–920.
- Monserud, R.A., Sterba, H., 1996. A basal area increment model for individual trees growing in even-and uneven-aged forest stands in Austria. *For. Ecol. Manage.* 80 (1–3), 57–80.
- Nothdurft, A., Engel, M., 2020. Climate sensitivity and resistance under pure- and mixed-stand scenarios in Lower Austria evaluated with distributed lag models and penalized regression splines for tree-ring time series. *Eur. J. Forest Res.* 139, 189–211.
- Nothdurft, A., Vospernik, S., 2018. Climate-sensitive radial increment model of Norway spruce in Tyrol based on a distributed lag model with penalized splines for year-ring time series. *Can. J. For. Res.* 48 (8), 930–941.
- Oberhuber, W., 2004. Influence of climate on radial growth of *Pinus cembra* within the alpine timberline ecotone. *Tree Physiol.* 24, 291–301.
- Oberhuber, W., Gruber, A., 2010. Climatic influences on intra-annual stem radial increment of *Pinus sylvestris* (L.) exposed to drought. *Trees* 24, 887–898.
- Plesa, I.M., González-Orenga, S., Al Hassan, M., Sestras, A.F., Vicente, O., Prohens, J., Sestras, R.E., Boscaiu, M., 2018. Effects of Drought and Salinity on European Larch (*Larix decidua* Mill.) Seedlings. *Forests* 9, 320.
- Pretzsch, A., 2014. Canopy space filling and tree crown morphology in mixed-species stands compared with monocultures. *For. Ecol. Manage.* 327, 251–264.
- Pretzsch, H., Biber, P., Schütze, G., Uhl, E., Rötzer, T., 2014. Forest stand growth dynamics in Central Europe have accelerated since 1870. *Nat. Commun.* 5, 4967.
- Pretzsch, H., Block, J., Dieler, J., Dong, P.H., Kohnle, U., Nagel, J., Spellmann, H., Zingg, A., 2010. Comparison between the productivity of pure and mixed stands of Norway spruce and European beech along an ecological gradient. *Annals Forest Sci.* 67, 712.
- Pretzsch, H., Schütze, G., Uhl, E., 2013. Resistance of European tree species to drought stress in mixed versus pure forests: evidence of stress release by inter-specific facilitation. *Plant Biol.* 15 (3), 483–495.
- R Core Team, 2020. R: A language and environment for statistical computing. R Foundation for Statistical Computing, Vienna, Austria <https://www.R-project.org/>.
- Rajczak, J., Pall, P., Schär, C., 2013. Projections of extreme precipitation events in regional climate simulations for Europe and the Alpine Region. *J. Geophys. Res.: Atmos.* 118 (9), 3610–3626.
- Rue, H., Martino, S., Chopin, N., 2009. Approximate Bayesian Inference for Latent Gaussian Models Using Integrated Nested Laplace Approximations (with discussion). *J. Roy. Stat. Soc.: Ser. B (Methodol.)* 71 (2), 319–392.
- Spiegelhalter, D.J., Best, N.G., Carlin, B.P., van der Linde, A., 2002. Bayesian measures of model complexity and fit. *J. Royal Stat. Soc.: Series B (Stat. Methodol.)* 64 (4), 583–639.
- Thomas, F.M., 2000. Growth and water relations of four deciduous tree species (*Fagus sylvatica* L., *Quercus petraea* Matt. Liebl., *Q. pubescens* Willd., *Sorbus aria* L. Cr.) occurring at Central-European tree-line sites on shallow calcareous soils: physiological reactions of seedlings to severe drought. *Flora* 195(2), 104–115.
- Timofeeva, G., Treydte, K., Bugmann, H., Rigling, A., Schaub, M., Siegwolf, R., Saurer, M., 2017. Long-term effects of drought on tree-ring growth and carbon isotope variability in Scots pine in a dry environment. *Tree Physiol.* 37 (8), 1028–1041.
- Toögo, M., Vallet, P., Tuilleras, V., Lebourgeois, F., Rozenberg, P., Perret, S., Courbaud, B., Perot, T., 2015. Species mixture increases the effect of drought on tree ring density, but not on ring width, in *Quercus petraea*-*Pinus sylvestris* stands. *For. Ecol. Manage.* 345, 73–82.
- Trouvé, R., Bontemps, J.-D., Collet, C., Seynave, I., Lebourgeois, F., 2017. Radial growth resilience of sessile oak after drought is affected by site water status, stand density, and social status. *Trees* 31, 517–529.
- Vanoni, M., Bugmann, H., Nötzli, M., Bigler, C., 2016. Drought and frost contribute to abrupt growth decreases before tree mortality in nine temperate tree species. *For. Ecol. Manage.* 382, 51–63.
- Vitali, V., Büntgen, U., Bauhus, J., 2018a. Seasonality matters — The effects of past and projected seasonal climate change on the growth of native and exotic conifer species in Central Europe. *Dendrochronologia* 48, 1–9.
- Vitali, V., Forrester, D.I., Bauhus, J., 2018b. Know your neighbours: drought response of Norway Spruce, Silver Fir and Douglas Fir in mixed forests depends on species identity and diversity of tree neighbourhoods. *Ecosystems* 21 (6), 1215–1229.
- Vitasse, Y., Bottero, A., Cailleret, M., Bigler, C., Fonti, P., Gessler, A., Lévesque, M., Rohner, B., Weber, P., Rigling, A., Wohlgemuth, T., 2019. Contrasting resistance and resilience to extreme drought and late spring frost in five major European tree species. *Glob. Change Biol.* 25 (11), 3781–3792.
- Watanabe, S., 2010. Asymptotic equivalence of Bayes cross validation and widely applicable information criterion in singular learning theory. *J. Mach. Learn. Res.* 11, 3571–3594.
- Zhang, J., Marshall, J.D., 1994. Population differences in water-use efficiency of well-watered and water-stressed western larch seedlings. *Can. J. For. Res.* 24, 92–99.